Talanta 306 (2026) 129728

Contents lists available at ScienceDirect

Talanta

journal homepage: www.elsevier.com/locate/talanta

Instrument-free quantitative colorimetric analysis using adsorption-band length in a packed silica gel column

Sychanh Phonxayxiong, Takashi Kaneta *

Department of Chemistry, Okayama University, 3-1-1 Tsushimanaka, Kita-ku, Okayama, 700-8530, Japan

ARTICLE INFO

Keywords:
Colorimetry
Distance-based detection
Silica gel
Adsorption

ABSTRACT

A simple and instrument-free colorimetric method for quantitative analysis is reported, in which analyte concentration is determined by measuring the length of a colored adsorption band formed in a packed silica gel column. The proposed method employs a miniature silica gel column that acts as a signal transducer after it adsorbs the colored compound from a solution during its flow in the column. The length of this band increases proportionally with analyte concentration, which enables quantitative detection via simple distance measurement. A theoretical model was developed to describe the relationship between solute concentration, adsorption behavior, and band propagation along the column. The principle was validated via the detection of both iron ions and enzyme-mediated glutamic acid. For Fe^{2+} analysis, the *o*-phenanthroline complexation method shows a level of sensitivity comparable to that of conventional spectrophotometry, which enables an almost quantitative recovery of trace iron in tap water. The limit of detection (LOD) and the limit of quantification (LOQ) were estimated to be 0.20 μM and 0.60 μM for the proposed method and 0.23 μM and 0.70 μM for spectrophotometry, respectively. The approach was further extended to glutamate detection using a cascade reaction involving glutamate oxidase and horseradish peroxidase with *N*-benzoyl leucomethylene blue as the chromogenic substrate. The LOD and the LOQ of the proposed method were 0.08 and 0.25 μM, and both values are superior to the 0.24 μM and 0.73 μM obtained using a microplate reader. By integrating preconcentration with a distance-based readout, this method provides a simple yet highly sensitive analytical platform and establishes distance as a quantitative signal for colorimetric detection.

1. Introduction

Highly sensitive chemical detection typically relies on analytical instruments to convert chemical information into measurable signals, but the development of fundamentally different detection methods for quantitative analysis without instrumentation has been a significant challenge. Colorimetric analysis has long been a fundamental technique in analytical chemistry owing to its simplicity, low cost, and direct visual readout. In conventional practice, however, colorimetric quantification generally relies on spectrophotometric measurements, which provide precise optical absorbance values but require dedicated instrumentation and a controlled laboratory environment. These requirements limit applicability to point-of-need and resource-limited settings.

The recent use of instrument-free analytical platforms has garnered an increasing amount of attention as alternative systems that could be viable for on-site quantification [1–5]. Various portable photometers employing light-emitting diodes and photodiodes have been developed [6–13], and several commercial devices are now available. The sensitivity of these systems, however, has remained inferior compared with the use of laboratory-grade spectrophotometers. In parallel, microfluidic paper-based analytical devices (μPADs) have emerged as another promising platform for on-site analysis [14]. In colorimetric μPADs, analytical information can be encoded as changes in color intensity, reaction time, or distance [15–17]. Among these formats, distance-based colorimetric methods—in which analyte concentration is given by the physical length of a color change—have gained particular interest because of the availability of intuitive and robust readouts [18–22].

Distance-based quantification has been predominant in μPADs, where a capillary-driven flow transports analytes along hydrophilic paper channels to generate colored species. This approach converts concentration into a measurable distance that can be read either directly by the naked eye or with simple imaging tools. Cate et al. introduced one

This article is part of a special issue entitled: FA-XVI 2025 published in Talanta.

* Corresponding author.
E-mail address: kaneta@okayama-u.ac.jp (T. Kaneta).

https://doi.org/10.1016/j.talanta.2026.129728
Received 7 January 2026; Received in revised form 12 March 2026; Accepted 25 March 2026
Available online 26 March 2026

of the earliest examples — a distance-based paper device for glucose and metal ion determination [18]. Subsequent studies by Yamada, Citterio, and Henry further refined this concept through dip-and-read formats and color-screening designs to improve reproducibility and visual contrast [22]. Additional reports, such as a selective potassium assay by Gerold et al. have expanded the range of detectable analytes and highlighted the potential of distance-based readouts for quantitative analysis [23].

Despite these advances, paper-based distance detection continues to face inherent limitations. Capillary flow in cellulose substrates is highly sensitive to variations in paper porosity, humidity, and surface chemistry, which often results in poor reproducibility. Moreover, most systems have been developed empirically and lack a rigorous theoretical framework that quantitatively links aspects such as solute concentration, transport behavior, and color-band formation. Limited sample capacity and the absence of intrinsic preconcentration mechanisms further constrain sensitivity, which is particularly true for trace-level analysis. These factors have hindered the broader analytical adoption of distance-based systems, which is particularly the case for applications requiring quantitative accuracy and mechanistic understanding.

One strategy that could be used to enhance sensitivity in portable colorimetric devices involves the adsorption of colored products onto solid materials. Kuramitz and co-workers reported a colorimetric method based on solid-phase extraction and sedimentation of particles that adsorb a colored product [24–27]. In this approach, analyte concentration is determined by measuring the accumulated color intensity of the solid phase. Although adsorption enhances sensitivity, data acquisition typically requires image capture under uniform illumination conditions that must be carefully controlled.

Another approach employs a microscope slide coated with silica gel, on which a colored product forms a band that enables distance-based quantification [28]. This principle is analogous to solute retention in thin-layer chromatography. While this method has achieved a higher level of sensitivity than that of conventional paper-based distance detection, measurement requires prolonged flow times of 35–40 min for 400 μL of a sample solution to traverse the thin-layer screen printed on the slide.

In a related study, Wang et al. reported a polydimethylsiloxane microchip device that integrates sample metering, on-chip reactions, gravitational and magnetic separation, and a distance-based visual readout for the quantification of multiple heavy metal ions in order to achieve sub-micromolar detection limits [29]. These approaches, however, have largely been limited to inorganic analytes such as metal cations and inorganic anions.

To address these challenges, we propose a distance-based colorimetric detection strategy that employs a miniature silica gel-packed column as a signal transducer. As a solution flows through the column, colored species are adsorbed onto silica particles that form a visible color band with a length that is directly correlated to analyte concentration. In contrast to the use of paper-based substrates, the packed silica medium provides controlled flow and well-defined adsorption dynamics that generate precise, reproducible, and tunable signals. A theoretical model was further developed to quantitatively describe the relationship between solute concentration, adsorption behavior, and color-band propagation, thereby establishing a general framework for distance-based quantification.

The versatility of this principle was demonstrated through two representative applications. First, Fe^{2+} ions were detected via the *o*-phenanthroline complexation reaction, which exhibited sensitivity as high as that of conventional spectrophotometric methods and enabled trace-level determination of Fe^{2+} in tap water with an almost quantitative level of recovery. Second, an enzyme-coupled assay for L-glutamic acid was demonstrated using a cascade reaction involving glutamate oxidase and horseradish peroxidase (HRP), with *N*-benzoyl leucomethylene blue (BLMB) serving as the chromogenic substrate [30,31]. Given the broad applicability of HRP-based assays, this example highlights the general utility of the proposed detection strategy.

Overall, the proposed system integrates adsorption-based preconcentration with a distance-based readout to provide a highly sensitive, instrument-free, and theoretically grounded platform for colorimetric quantification. By extending distance-based analysis beyond paper devices, this work expands the scope of quantitative, low-cost chemical sensing.

2. Experimental

2.1. Materials and apparatus

All chemicals used in this study were of analytical grade. Deionized water (DI water, resistivity >18 MΩcm) was produced using an Elix water purification system (Direct-Q UV3, Merck, Darmstadt, Germany) for the preparation of all aqueous solutions. Ammonium iron (II) sulfate hexahydrate, *o*-phenanthroline (phen), sodium borate decahydrate, boric acid, hydrochloric acid (HCl), L-glutamic acid, horseradish peroxidase (HRP), and L-glutamate oxidase were all obtained from FUJIFILM Wako Pure Chemical Corporation (Osaka, Japan). Acetic acid and porous silica gel (Silica Gel 60 N (spherical, neutral), 63-210 μm) were purchased from Cica KANTO CHEMICAL CO., INC. (Tokyo, Japan). Sodium acetate dihydrate and L-ascorbic acid were obtained from NACALAI TESQUE, Inc. (Kyoto, Japan). *N*-Benzoyl leucomethylene blue (BLMB) was purchased from Tokyo Chemical Industry Co., Ltd. (Tokyo, Japan) and was dissolved in dimethyl sulfoxide. Syringes (1.5 mL, 10 mL, and 20 mL) were purchased from AS ONE Corporation (Tokyo, Japan). Solutions were flowed into the column either by hand-pressurizing the syringe manually or via an air pump (e-AIR, GEX Corporation, Osaka, Japan). The preparation and storage methods of enzyme solutions for glutamate assay are provided in the Supplementary Data (Supplementary Data, S1.1).

A UV-Vis spectrophotometer (Shimadzu, Kyoto, Japan, UV-2400 PC) and a microplate reader (SYNERGY, Agilent BioTek, Tokyo, Japan) were used for colorimetric analysis to validate this proposed method. Images were captured using a smartphone camera (Vivo Y11) under ambient light in a room. The captured images were processed using ImageJ software. A 3D printer (Da Vinci Jr. Pro, XYZ Printing, Tokyo, Japan) was used to fabricate a cap to close the end of the column, which was designed using Autodesk Fusion software. The retention behavior of a solute in a silica gel column was simulated by calculations using Python programming language.

2.2. Column preparation

Plastic tubes made of poly (methyl 2-methylpropenoate) with an inner diameter of 1.0 mm were cut to lengths of 50 mm and used as miniaturized columns. The outlet of each column was closed with a small piece of cotton and a cap fabricated using a 3D printer to prevent silica gel from escaping. Silica gel particles (30 mg) were suspended in 4 mL of Milli-Q water and then loaded into the tube using a 2.5-mL syringe. The tube was gently tapped to ensure uniform packing. The packed column was washed with 2 mL of a 1 M concentration of HCl and subsequently rinsed with 2 mL of Milli-Q water to remove any residual cations from the silica gel surface.

2.3. Analytical procedure

The detection scheme for the distance-based readout is illustrated in Fig. 1. Fig. 1A shows the components of the detection column, while Fig. 1B features the fabricated flow device. Either a 10- or 20-mL disposable syringe was connected to the plastic column tube using polyvinyl Chloride, PTFE, and silicone tubing, as depicted in Fig. 1B. The procedure for introducing the sample solution appears in Fig. 1C.

Before sample loading, the column was pretreated with 1 M HCl. Sample solutions were prepared either using a colorimetric reaction that

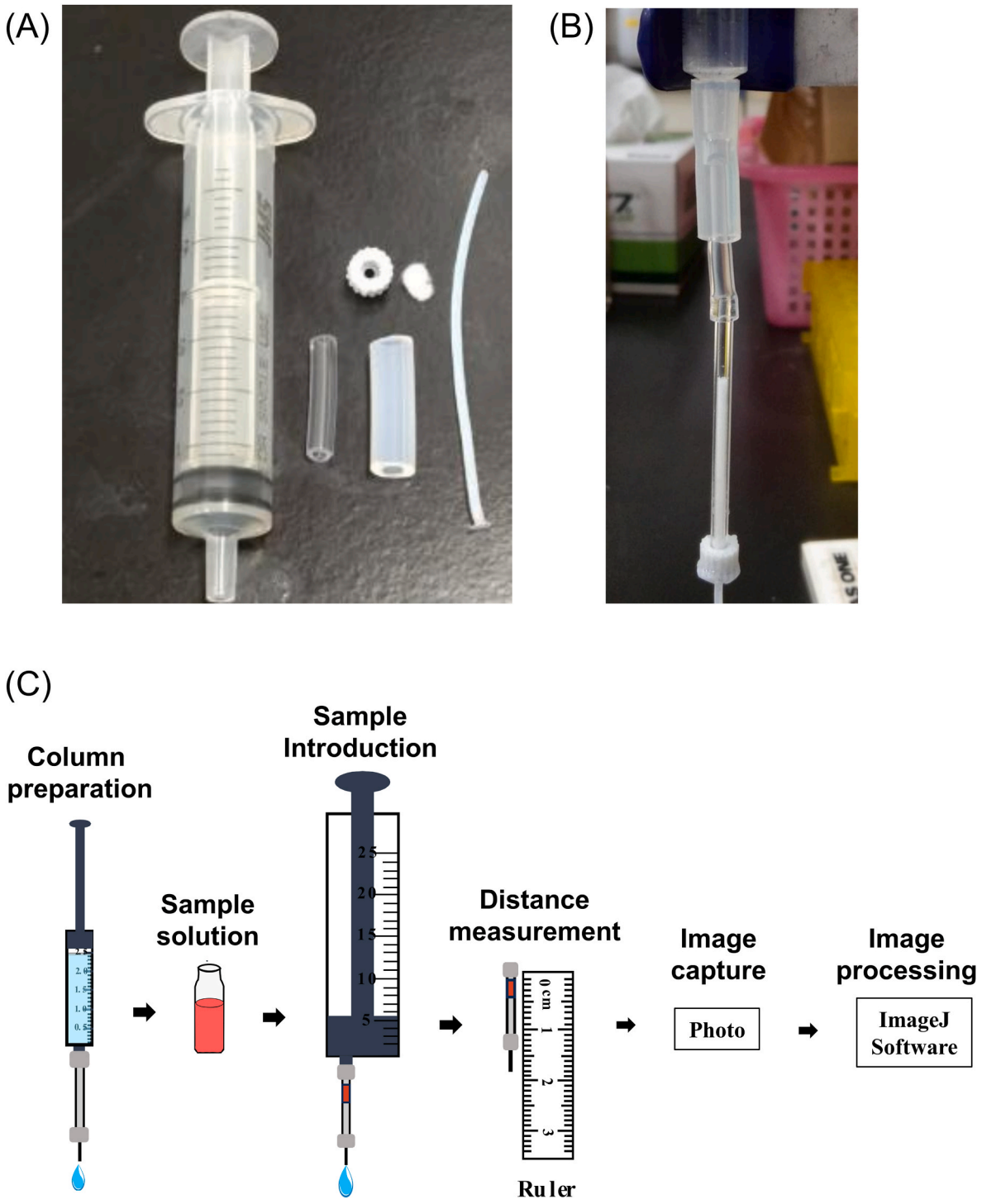

Fig. 1. The equipment used for distance-based detection.
(A) parts, (B) fabrication of the miniaturized column, and (C) schematic illustration of the operation.

produced a colored $Fe(phen)_3^{2+}$ complex (for Fe^{2+} measurement) or via an enzyme-coupled reaction using a chromogenic substrate (for glutamate measurement). The resultant solutions were introduced into the miniaturized column manually via hand pressure or by using an air pump with the flow rate adjusted to 1.0 mL min^{-1}. The flow rate with hand pressure was adjusted by observing the number of droplets discharged from the outlet tube. When flowing 1 mL of a solution into the column, 47 ± 1 (n = 3) droplets were ejected from the outlet tube. Thus, we controlled the injection of the solution to discharge approximately one drop every 1.3 s while watching a timer. The total time required to introduce 1 mL of the solution is estimated to be 61.1 s using this method. Thus, the last droplet was ejected quickly to adjust the flow rate to 1 mL min^{-1}. We could adjust the flow rate to 0.99 ± 0.3 mL min-1 (n = 3) using this method. After the solution was completely flushed out with air, the length of the colored band formed inside the miniaturized column was measured using a ruler and ImageJ software.

In the image-processing step, the color intensity of the colored band was plotted as a function of the distance from the edge of the silica gel. The distance corresponding to a given concentration was defined as the mid-point between the positions of the maximum and minimum average

intensities. This distance was then plotted against the analyte concentration to generate a calibration curve.

The reaction conditions for Fe^{2+} analysis were as follows: Fe^{2+} standard solutions (10 mL, 0.125–2.0 μM) were placed in 20 mL glass vials, after which 0.4 mL of 2.5% (w/v) L-ascorbic acid solution was added. The solutions were let stand for 60 s, and then 0.4 mL of sodium acetate buffer (pH 4.7) and 0.2 mL of a 30 mM concentration of phen solution was added. The pH of each mixture was then adjusted to 8.5 by adding sodium borate buffer (pH 9.0). The total volume of the sample solutions was 13.4 mL after the pH adjustment.

The principle of the glutamate measurement followed a method previously reported by our group [30,31]. In the present study, the reaction was performed as follows: A 5 mL aliquot of L-glutamic acid standard solution (0.03–2.0 μM) was transferred into a glass vial. Subsequently, 50 μL of a 1000 μM concentration of BLMB dissolved in a solution of dimethyl sulfoxide, 50 μL of a 100 mg L^{-1} concentration of HRP, and 50 μL of an 80 mg L^{-1} concentration of L-glutamate oxidase were each added in a sequential manner. The mixture was allowed to react for 30 min at room temperature, after which 100 μL of borate buffer (pH 9.0) was added to adjust the pH to 8.5. The total volume of the sample solutions was 5.25 mL after the pH adjustment.

The resultant solution was then introduced into the column at a flow rate of 1 mL min^{-1}. After the solution was completely expelled with air, the distance of the colored band was determined by processing the image using ImageJ software. The resultant solutions were also used to measure absorbance via a microplate reader. Then, 200-μL of each solution was added to the well of a microtiter plate to measure the absorbance at 668 nm.

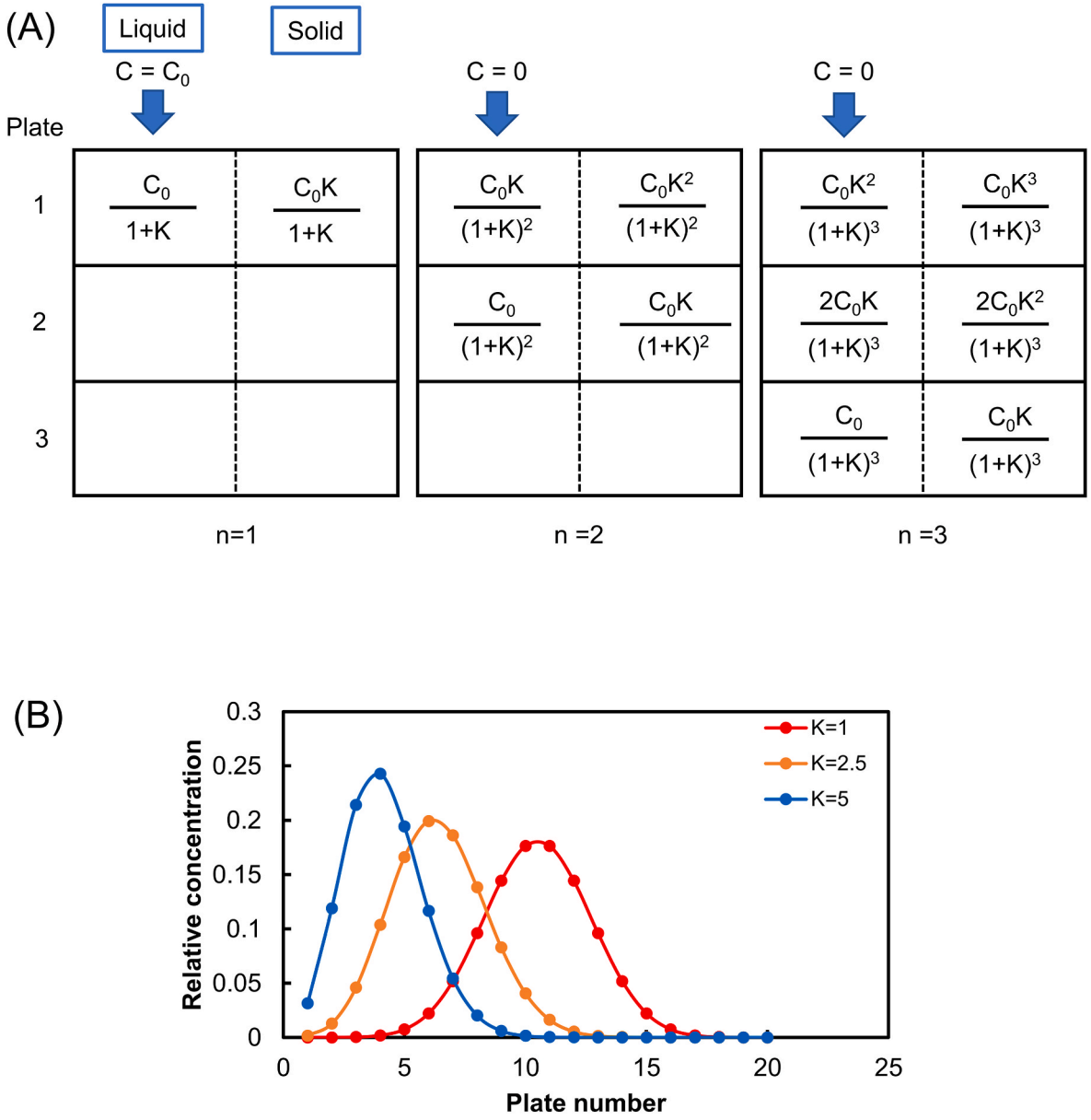

Fig. 2. Models of retention in the column.
(A) and (B) A model and distribution of a solute in chromatography; The solute is introduced into the column and flushed by liquid without the solute. (C) and (D) A model and distribution of a solute in the proposed method for distance-based detection; The solute is introduced into the column successively and flushed by liquid containing the solute. $C_0 = 1$, plate number is set to 20. The graph was calculated by assuming that the concentration in the solid phase is lower than the maximum adsorption capacity of the solid phase (the solid phase is not saturated with the solute in the first plate).

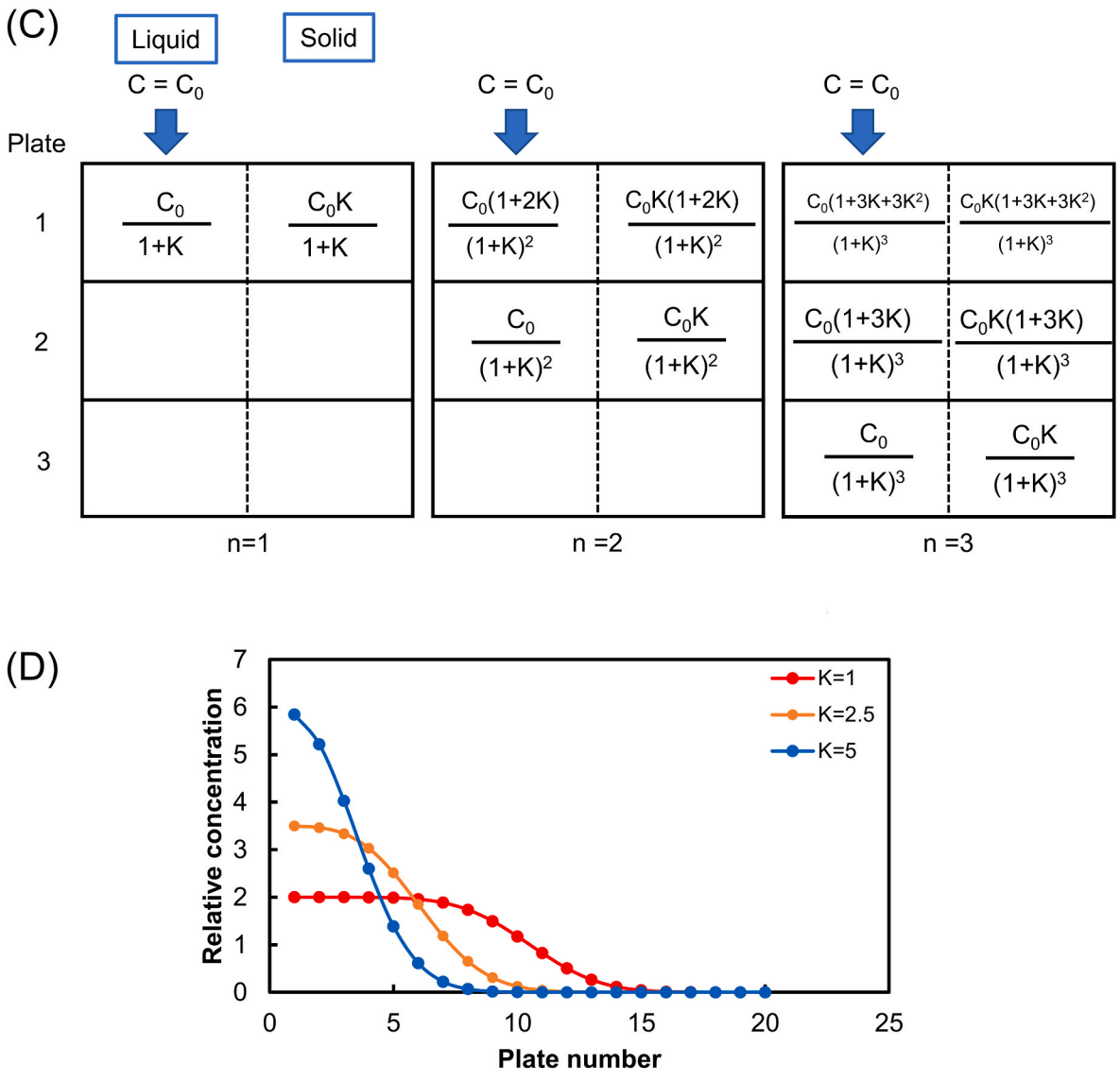

Fig. 2. (*continued*).

3. Results and discussion

3.1. Theory

The analytical principle of the present method is based on the accumulation of a colored analyte in a solid phase, which results in the formation of a visible color band along a packed column. To rationalize this behavior, we developed a theoretical model that would approximate chromatographic plate theory. In classic plate theory, separation processes—such as countercurrent extraction using a Craig apparatus—are described as sequences of discrete equilibration steps. By analogy, the packed column in the present system is conceptually divided into a series of theoretical plates, each attaining the minimum segment of adsorption equilibrium between the aqueous and solid phases [32].

Within each plate, the solute is assumed to be distributed between the aqueous and solid phases according to a constant distribution coefficient (K). The total number of plates (n) thus provides a measure of the axial distance along the column and serves as a dimensionless representation of band length.

To establish a reference model, a conventional chromatographic retention process was first considered (Fig. 2A, $n = 3$). For simplicity, the volumes of the aqueous and solid phases in each plate were assumed to be identical. The initial concentration (C_0) of a solute was introduced with a distribution coefficient (K) into the first plate as an aqueous solution, which was then followed by a continuous introduction of a solute-free aqueous solution. This process is mathematically equivalent to successive solvent extraction in the Craig method.

The solute concentrations in the aqueous and solid phases of plate i after n equilibration steps are denoted as $Ca_{q,i}^{(n)}$ and $C_{s,i}^{(n)}$, respectively, and are described by equations (1) and (2).

$$C_{aq,i}^{(n)} = C_0 \frac{\binom{n-1}{i-1} K^{n-i}}{(1+K)^n} \tag{1}$$

$$C_{s,i}^{(n)} = K C_{aq,i}^{(n)} \tag{2}$$

Fig. 2B shows calculations for the solute distribution across the plates for $n = 20$ and $C_0 = 1$. As the distribution coefficient decreases, the interaction between the solute and the solid phase weakens, which leads to an increase in the migration distances and to a broader range of concentration profiles, which is classic chromatographic behavior.

Unlike the single introduction of a sample solution, the present method continuously introduces a constant concentration (C_0) of sample solution containing the analyte. This difference in boundary conditions

results in a distinct behavior for solute distribution. The corresponding model for n = 3 is illustrated in Fig. 2C. Initially, the sample solution enters the first plate, which is followed by equilibration between the aqueous and the solid phases. The equilibrated aqueous solution moves to the second plate while the sample solution with the concentration of C_0 enters the first plate. Both the first plate and the second plate are independently equilibrated between the aqueous phase and the solid phase.

As the solution flows successively through the column, adsorption equilibrium is established within each plate. The solute distribution along the column is described by equations (3) and (4).

$$C_{aq,j}^{(n)} = C_0 \frac{\sum_{i=0}^{n-j} \binom{n}{j} K^i}{(1+K)^n} \tag{3}$$

$$C_{s,j}^{(n)} = K C_{aq,j}^{(n)} \tag{4}$$

In equations (3) and (4), j denotes the plate number. Fig. 2D shows simulated concentration profiles for $n = 20$. Under this idealized assumption, solutes with larger K values exhibit stronger retention, which forms shorter bands that are more localized. However, this model assumes an infinite adsorption capacity of the solid phase and consequently overestimates solute accumulation in the upstream plates, particularly for larger K values.

To more practically represent experimental conditions, the finite adsorption capacity of the solid phase was incorporated into the model. A maximum solid-phase concentration, $C_{s,max}$, was introduced, beyond which additional solute in the aqueous phase is assumed to pass through the solid phase without adsorption. In the present simulations, $C_{s,max}$ is set to 1, which is the same as the inlet concentration, C_0. Fig. 3A shows simulated concentration profiles under this constraint. When K is small, the solute preferentially remains in the aqueous phase, and this results in a higher level of aqueous-phase concentration as well as to a broader range of band profiles. As K increases, adsorption becomes more favorable, and this leads to a progressive elongation of the band where $C_s = 1$. It is important to note that the incorporation of a finite level of adsorption capacity prevents unrealistic levels of overaccumulation. The maximum relative concentration is 2 ($C_{aq} = 1$ and $C_s = 1$) because the aqueous solution remains in the column, as depicted in Fig. 3A.

In practical operations, the distribution coefficient (K) for a given analyte remains constant while sample solutions of varying concentrations are introduced into the column. To simulate this situation, concentration profiles were calculated assuming $K = 5$, $C_0 = 1$, and $C_{s,max} = 1$ (Fig. 3B). In Fig. 3B, the aqueous solution is completely ejected from the column, so the relative concentration indicates the C_s of each plate. A Python script for the calculations in Fig. 3B is provided in the Supplementary data (Supplementary data, Python Script for calculation). The Python script includes the steps for the introduction and the ejection of the sample solution.

Under these conditions, the axial position corresponding to half of the maximum concentration ($C_0/2$) shifts systematically with analyte concentration. Consequently, the analyte concentration can be quantitatively determined by the length of the colored band formed in the column. As shown in Fig. 3C, the relationship between analyte concentration and band length, expressed in terms of plate number, is approximately linear at low concentrations, but deviates from linearity at higher concentrations when adsorption capacity reaches saturation.

3.2. Optimization of conditions for adsorption

In this study, silica gel plays the role of a solid phase to form a band where a colored analyte accumulates via a strong adsorption capability. In the present study, two reactions, the complexation of Fe^{2+} with phen and an enzymatic reaction for glutamate detection using BLMB as the substrate, were employed to prove the concept of the proposed method.

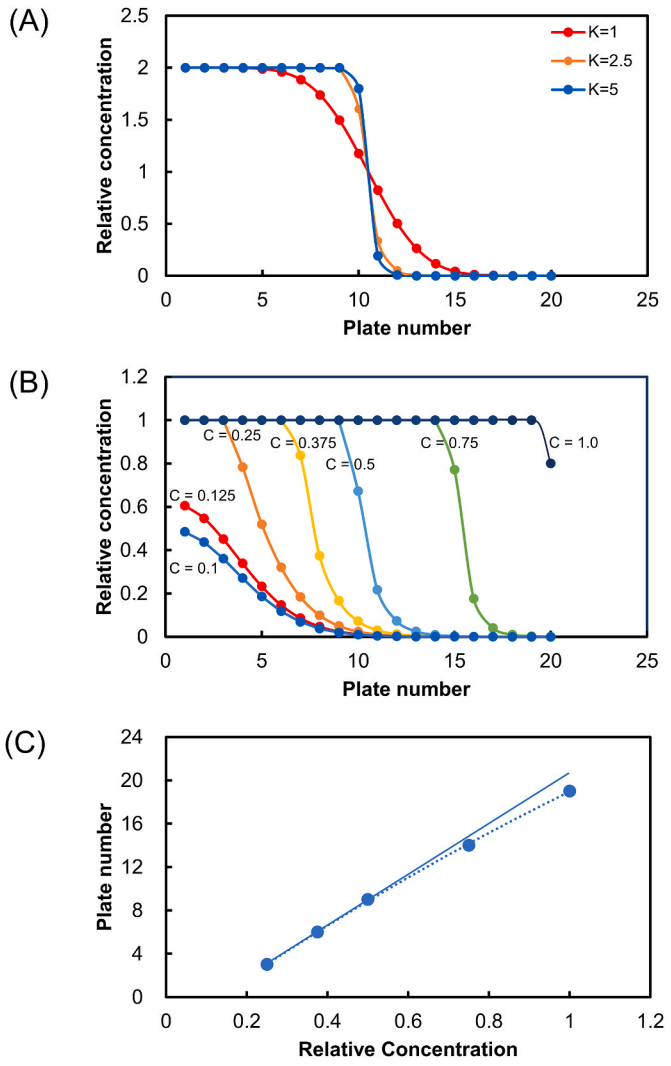

Fig. 3. Simulation of the solute distribution in the column.
The sample concentration, C_0, and the maximum concentration in the solid phase, $C_{s,max}$, are set to 1. (A) The sample solution remains in the column, so the concentration expresses the total concentration of the solute in the liquid and solid phases (the sample solution is not flushed out from the column). (B) Different concentrations of the solution flowed into the column; The solution is completely flushed out by air, so the concentration expresses the concentration of the solute in the solid phase. (C) Dependence of the distance at $C = 0.5C_0$ on the solute concentration when the plate number is set to 20.

In the complexation reaction, Fe^{2+} forms a red-colored complex, $Fe(phen)_3^{2+}$, while the enzymatic reaction generates cationic methylene blue from BLMB. Preliminary tests confirmed that both colored products had strongly adsorbed onto the surface of silica gel.

In distance-based detection, the column serves both as an accumulation medium and a detector of colored products. The method was first applied to the determination of Fe^{2+}. Because silica gel dissociates protons to generate negatively charged functional groups, the pH of the sample solution influences the adsorption capacity of silica gel.

To optimize the pH for retaining the Fe^{2+} reaction product, $Fe(phen)_3^{2+}$, the pH of the solution was adjusted to within a range of between 6.0 and 9.5 using sodium borate as a buffer. The relationship between the solution pH and the distance of the colored band is shown in Fig. S1 of the Supplementary data. A shorter band distance indicates stronger adsorption onto silica gel; thus, $Fe(phen)_3^{2+}$ was most efficiently adsorbed at pH values between 8 and 9, with the shortest distance observed at pH 8.5. The enhanced adsorption efficiency under mildly basic conditions could be attributed to the dissociation of silanol

(Si–OH) groups, which form negatively charged siloxide sites (Si–O$^-$). These sites electrostatically interact with cationic species — in particular, the $Fe(phen)_3^{2+}$ complex [24,33]. Accordingly, pH 8.5 was chosen as the optimal pH for subsequent experiments.

The optimal pH obtained in this study is slightly higher than that reported for the sedimentation-based method using silica gel, where the maximum adsorption of $Fe(phen)_3^{2+}$ occurs at pH 7.0 [24]. However, the adsorption of metal 1-(2-pyridylazo)-2-naphthol (PAN) that complexes onto modified silica gel is known to reach its highest level at pH 8.5 [34], which is consistent with our results. By contrast, as shown in Fig. S2 of the Supplementary data, band broadening was observed at pH 9.5. The $Fe(phen)_3^{2+}$ complex is reported to be stable within a pH range of from 2 to 9 [35]. A pH higher than 9 could cause a ligand substitution between hydroxide ions and phen molecules. The ligand substitution with hydroxide ions reduces the positive charge of the iron complex and weakens its interaction with silica gel. The other reason for the band broadening at pH 9.5 would be attributed to an increase in the concentration of sodium ions. In the present study, sodium borate was used to increase the pH of the sample solution. Thus, the concentration of sodium ions increases with increases in the pH. A high concentration of sodium ions would prevent the interactions of other cationic species with silica gel, which could possibly result in a band broadening of the complex. Thus, the band broadening at pH 9.5 could be attributed to an increase in ionic strength, which would alter the adsorption behavior.

The flow rate influences the band distance because adsorption requires a certain amount of time to achieve equilibrium. Table S1 of the Supplementary data displays the effect of the flow rate. As speculated, a low flow rate efficiently accumulates the colored product and decreases the distance of the colored band due to an enhanced level of adsorption efficiency. Furthermore, the reproducibility indicated by the standard deviation is also small when the flow rate is reduced. However, a low flow rate extends the time required for analysis, and this necessitates a compromise between reproducibility and analysis time. In the present study, the flow rate was adjusted to 1.0 mL min^{-1}, which required 10 min to flow 10 mL of a sample solution.

It should be noted that the relative standard deviations (RSDs) of the distances were less than 5% (1.0% and 3.3% at flow rates of 0.7 and 1.0 mL min^{-1}, respectively), even when the flow rate was controlled using the hand-pressure method. The distance is influenced by several factors such as the flow rate, the sample volume, the chemical reaction, and other experimental conditions. Nevertheless, the hand-pressure method provides good reproducibility, with RSDs lower than 5%. Conversely, the air pump used in this study did not control the flow rate precisely, which resulted in no improvement in the reproducibility of the distance. When the pump pressure was adjusted to the minimum level, the flow rate was 0.53 ± 0.08 mL min^{-1} (n = 18, RSD = 15%). Under these conditions, the RSDs of the distances at six different iron concentrations were 8–15% (n = 3 for each concentration), which were considerably larger than those obtained with the hand-pressure method. These results indicate that the hand-pressure method provides good reproducibility of the color-band distance when the flow rate is adjusted to below 1 mL min^{-1}.

3.3. Analytical feature of Fe^{2+} ions and application to real samples

Standard solutions of Fe^{2+} (10 mL) with concentrations ranging from 0.125 to 2.0 μM were prepared to construct calibration curves for both distance-based colorimetry using image processing and spectrophotometry. After the reaction, the solutions were flowed into the column for distance-based colorimetry, whereas their absorbances were measured at 510 nm for spectrophotometry. The calibration curve in the distance-based colorimetry and images of the columns are shown in Fig. 4A. Conversely, concentrations of 0.125 μM are undetectable in spectrophotometry, so the calibration curve was constructed within a range of 0.5 to 2.0 μM, as shown in Fig. 4B. The calibration curves yielded regression equations of D = (1.47 ± 0.08)C + 2.08 ± 0.04 with a

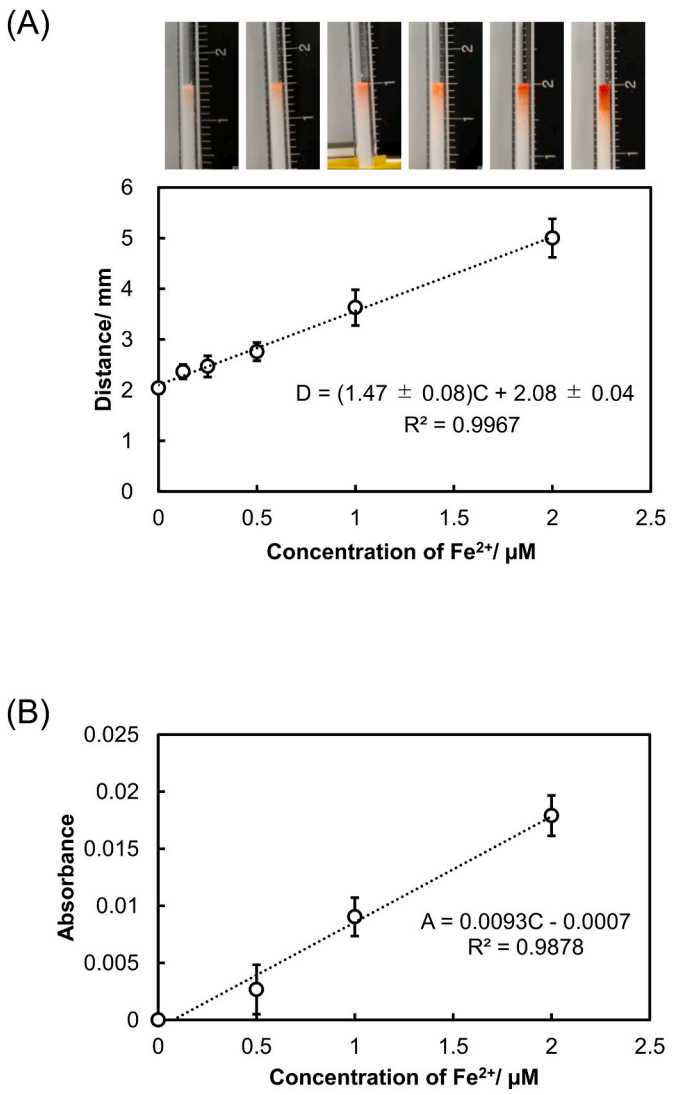

Fig. 4. Calibration curves of Fe^{2+} obtained using a standard absorption spectrophotometer and that using the proposed method for distance-based detection: (A) Spectrophotometry, (B) distance-based detection. Images in (B) show the retention of $[Fe(phen)_3]^{2+}$ in the silica gel column. The reaction conditions are shown in the text.

coefficient of determination (R^2) of 0.9967 for the distance-based colorimetry and A = 0.0093C - 0.0007 with R^2 of 0.9878 for spectrophotometry. The linearity seemed better for the results from distance-based colorimetry than for those from spectrophotometry at such a low level of concentration.

The limits of detection (LOD) and quantification (LOQ) for the proposed distance-based detection method were estimated to be 0.20 μM and 0.60 μM, whereas those for conventional spectrophotometry were 0.23 μM and 0.70 μM, respectively, as calculated using the method proposed by Olivieri [36] where calibration parameters such as slope, residual standard deviation, blank leverage, and number of samples are included in their estimation. Thus, distance-based colorimetry provides detectability that is comparable to that of instrument-based spectrophotometry.

Further enhancement of sensitivity could be achieved by increasing the sample volume that is introduced into the column, although this would inevitably extend the analysis time. In our previous study, a distance-based μPAD achieved a low LOD of 20 ppb (0.36 μM) for Fe^{2+} by introducing 1 mL of sample solution [21]. However, because the flow relied solely on spontaneous capillary action, processing 1 mL required

9–12 h. By contrast, the present method employs active flow control, which allows 10 mL of a sample solution to be processed within 10 min at a flow rate of 1.0 mL min^{-1}. This represents a substantial improvement in analytical throughput while maintaining high sensitivity.

Distance-based detection relies on the adsorption of cationic species onto silica gel. Therefore, the presence of other cations in the sample solution could inhibit the adsorption of the target analyte. To evaluate potential interferences in the measurement of Fe^{2+}, various species were examined, as shown in Fig. S3. The tested interferents included Mn^{2+}, Ni^{2+}, Cu^{2+}, Cd^{2+}, Cr^{3+}, Pb^{2+}, Zn^{2+}, and several salts ($MgSO_4$, $CaCl_2$, Na_2CO_3, Na_2SO_4). When 2 μM Fe^{2+} samples contained equal concentrations (2 μM) of different foreign metal ions, the measured distance showed no significant change, and relative standard deviations (RSDs) fell to within ±7.0%. This level of variation is acceptable because tolerance concentrations are defined as the highest concentrations of interfering species that will produce a change of less than 10% in the analytical response for Fe^{2+} [37].

However, when a mixture of seven metal ions (total concentration: 14 μM) was added to a 2 μM Fe^{2+} sample, a noticeable effect was observed. Sodium ions showed no detectable influence on the band distance, whereas calcium and magnesium ions reduced the adsorption of $Fe(phen)_3^{2+}$, which resulted in a 23.6% increase in band length. Therefore, heavy metal ions must either be removed or masked when their concentrations are significantly higher than that of Fe^{2+} in the sample. Furthermore, alkaline earth metal ions, Mg^{2+} and Ca^{2+}, could require either removal or masking if the sample contains them at concentration levels of several μM — for example, precipitation formation with either carbonate or oxalate could remove the interference of alkaline earth metal ions.

Results from both inter- and intra-day reproducibility were also examined using a standard solution of 2 μM Fe^{2+}. The RSDs of the distance exhibited 6.1% at n = 5 for one day and 6.2% at n = 5 after five days. The RSDs were slightly higher than 5%, but there was no difference even for different days. The slightly poor reproducibility was likely due to insufficient control of the flow rate, which could be adjusted either manually or by using an air pump. If a more precise pumping system was used, the reproducibility could be improved.

The proposed method was also applied to the determination of Fe ions (total of Fe^{2+} and Fe^{3+}) in tap water collected from different rooms, as summarized in Table 1. Among these samples, spectrophotometry detected Fe ions only in sample 4 of the tap water, because the Fe ion concentrations in the other samples were below the limit of detection. To validate the proposed method, we used a *t*-test to evaluate the results. The differences between the proposed method and spectrophotometry were assessed at the 95% confidence level, and a p-value greater than 0.05 ($p > 0.05$) was interpreted as indicating that there was no statistically significant difference between the methods. The value obtained for the tap water sample 4 showed excellent agreement between the proposed distance-based method and spectrophotometry, with no significant difference observed between the two techniques.

Table 1
Determination of iron ions in tap water samples.

Sample	Found/μM		Relative error	p-value
	Distance-based detection (n = 3)	Spectrophotometry (n = 3)		
Tap water 1	0.38 ± 0.11	ND	-	
Tap water 2	0.25 ± 0.10	ND	-	
Tap water 3	0.28 ± 0.03	ND	-	
Tap water 4	0.85 ± 0.07	0.94 ± 0.00	−0.09	0.149
Tap water 5	0.53 ± 0.05	ND	-	

The values are expressed as the mean ± SD (n = 3). ND: Not detected.

Tap water samples 2 and 3 contained Fe ions at concentrations that approximated the LODs for both methods; however, the absorbance values measured by spectrophotometry could not be distinguished from the blank, which indicated that the concentrations were below the LOD. These findings suggest that, although spectrophotometry exhibits smaller standard deviations, the proposed distance-based method provides superior detectability and is capable of measuring Fe ion levels that lie below the LOD for conventional spectrophotometry.

The recovery test provided acceptable results that are comparable to those obtained using conventional spectrophotometry. Both the results with and without spiking showed good agreement between distance-based colorimetry and conventional spectrophotometry, which gave recoveries of 97.2 to 116.0%, respectively, as shown in Table 2.

3.4. Analytical feature of glutamate and application to real samples

To extend the applicability of distance-based colorimetry, an enzymatic reaction using BLMB as a substrate was employed for the determination of glutamic acid [31]. The reaction was based on the production of hydrogen peroxide in the oxidation of glutamic acid, and was followed by the colorimetric reaction of BLMB in the presence of HRP. This reaction suggests wide applicability because the colorimetric reaction could support any enzymatic reactions that generate hydrogen peroxide.

Within a concentration range of 0.03 to 2.00 μM of glutamic acid, the calibration curves were constructed via both distance-based colorimetry and spectrophotometry using a microplate reader. The calibration curve of the proposed method for distance-based colorimetry exhibited excellent linearity as shown in Fig. 5A ($D = (2.24 \pm 0.17)C + 1.69 \pm 0.06$, $R^2 = 0.9990$). At 2.00 μM, however, the measured distance deviated from the linear trend, which is consistent with the behavior predicted by the simulation discussed in the Theory section. The calibration curve obtained using the microplate reader also showed a good linear relationship within a range of 0.03 to 2.00 μM, which is given in Fig. 5B ($A = 0.0399C + 0.0025$, $R^2 = 0.991$).

Values for LOD and LOQ were calculated based on the calibration curve shown in Fig. 5A at 0.08 and 0.25 μM, respectively. These values are lower than those obtained using a microplate reader, which estimated LOD of 0.24 μM and LOQ of 0.73 μM based on the calibration curve shown in Fig. 5B. The results clearly demonstrate that the proposed method for distance-based colorimetry is compatible with enzyme-coupled reactions employing HRP and BLMB as the enzyme and chromogenic substrate, respectively, and is as sensitive as that of spectrophotometry when using a microplate reader, although the linear range is slightly narrower.

To demonstrate the practical applicability of distance-based colorimetry in the determination of enzymatic reactions, we measured the levels of glutamic acid in several food samples, as shown in Table 3. Although the error of a dashi sample is slightly larger than those of miso samples, the values from the proposed method for distance-based colorimetry were in good agreement with those determined using a

Table 2
Recovery test for tap water samples.

Method		Spiked concentration/μM		
		0	0.2	0.4
Distance-based detection	Found/μM	0.38	0.63	0.90
	Recovery/%	-	108.6	116.0
Spectrophotometry	Found/μM	0.49	0.70	0.87
	Recovery/%	-	101.2	97.2

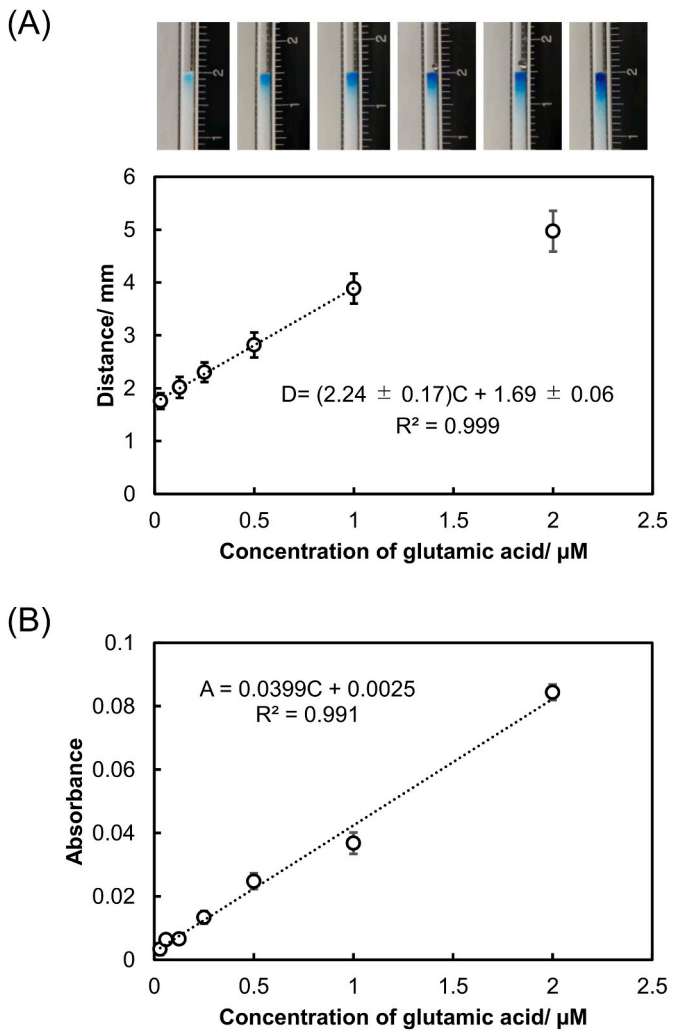

Fig. 5. Calibration curves of glutamic acid obtained using a microplate reader and that using the proposed method for distance-based detection: (A) Distance-based detection, (B) microplate reader. Images in (B) show the retention of methylene blue, which was produced by the enzymatic reaction, in the silica gel column. The reaction conditions are shown in the text. (For interpretation of the references to color in this figure legend, the reader is referred to the Web version of this article.)

Table 3
Determination of L-glutamate in food samples.

Sample	Found/mM		Error	p-value
	Distance-based detection (n = 3)	Microplate reader (n = 2)		
Dashi	2.31 ± 0.55	1.70 ± 0.05	+0.61	0.20
Miso 1	1.38 ± 0.22	1.18 ± 0.01	+0.20	0.26
Miso 2	1.58 ± 0.44	1.59 ± 0.10	−0.01	0.91

The values were expressed by mean ± SD.

microplate reader (spectrophotometric method), as suggested by the p-values larger than 0.05 at a 95% confidence interval. These results indicate that distance-based detection has wide applicability to enzymatic assays that generate hydrogen peroxide and are measured via colorimetry using HRP as the enzyme and BLMB as the substrate.

3.5. Advantages and limitations

The proposed method for distance-based colorimetry offers several notable advantages: straightforward operation, the use of readily available and low-cost materials, good portability, and high sensitivity comparable to that obtained using a conventional spectrophotometer with a microplate reader. It should be emphasized that the LODs of the proposed method approximate those of a spectrophotometer with a microplate reader. These features expand the possibility of on-site applications and sensitive detection in poorly equipped laboratories.

However, the proposed method includes certain limitations. One of these is that the attainment of a high level of reproducibility requires a precise pumping system, which in turn increases the overall cost of the device, which necessitates a compromise between affordability and analytical precision. In addition, the proposed approach is applicable primarily to colored cationic species that exhibit strong adsorption onto silica gel. This limitation in analyte scope could be resolved by employing alternative adsorbents, such as anion- or cation-exchange materials or hydrophobic solid supports (e.g., octadecylsilane), which would broaden the range of detectable species and enhance the versatility of the method. Furthermore, it would be attractive if materials could selectively adsorb a colored analyte, such as either a molecularly imprinted polymer or a solid support modified with a molecular recognition element.

Image acquisition and processing represent additional sources of experimental variability, particularly due to differences in illumination conditions and operator handling. To evaluate the robustness of the proposed method against such variations, we measured the band distance using photographs taken under different lighting conditions (Fig. S4, Supplementary data). For each image, the distance from the column inlet to the position corresponding to half of the maximum red intensity was determined in pixels. The measured distances yielded a mean value and standard deviations of 336 and 28 pixels (RSD = 8.4%), respectively. Although 5% of RSD is recommended for precise analysis in the equipped laboratories, 8.4% would be acceptable for on-site analysis. However, a portable photo studio could improve the reproducibility if available.

4. Conclusions

We have developed a novel colorimetric detection method that is based on the adsorption of colored reaction products onto silica gel packed within a miniaturized column. The theoretical model presented in this study successfully describes the retention behavior in the column and supports the observed dependence of the colored band length on the concentration of the reaction product. The proposed method was applied to the determination of iron ions in tap water and glutamic acid in food samples, and the results were in good agreement with those obtained using conventional absorption spectrophotometry and microplate reader-based assays. Although the precision of the proposed distance-based approach is lower than that of instrument-based spectrophotometry, its LODs are comparable and are much lower than those of portable devices such as PADs and portable photometers, because the analytical process includes the accumulation of colored products. The enzymatic reaction employed herein demonstrates the excellent applicability of this approach for broader enzymatic assays using HRP, which is widely applicable in biochemical analysis. While the present study was focused on cationic species, future work will extend the method to anionic and hydrophobic analytes by employing either modified silica gels or polymer-based adsorbents. Overall, the proposed distance-based colorimetric method provides a portable, inexpensive, user-friendly, and sufficiently sensitive platform for on-site and home-based chemical analysis.

CRediT authorship contribution statement

Sychanh Phonxayxiong: Writing – review & editing, Writing – original draft, Visualization, Validation, Methodology, Investigation, Formal analysis, Data curation. **Takashi Kaneta:** Writing – review &

editing, Writing – original draft, Visualization, Supervision, Resources, Project administration, Methodology, Funding acquisition, Formal analysis, Data curation, Conceptualization.

Declaration of generative AI and AI-assisted technologies in the manuscript preparation process

The authors used ChatGPT to generate Python scripts for calculations in the section on Theory.

Declaration of competing interest

The authors declare that they have no known competing financial interests or personal relationships that could have appeared to influence the work reported in this paper.

Acknowledgments

This work was supported by the Japan Society for the Promotion of Science (JSPS), KAKENHI, Grant Numbers JP25K01800.

Appendix B. Supplementary data

Supplementary data to this article can be found online at https://doi.org/10.1016/j.talanta.2026.129728.

Data availability

Data will be made available on request.

References

[1] E.M. Khalaf, H.S. Jabbar, R.M. Romero-Parra, G.R.L. Al-Awsi, H.S. Budi, A. S. Altamimi, M.A. Gatea, K.T. Falih, K. Singh, K.A. Alkhuzai, Smartphone-assisted microfluidic sensor as an intelligent device for on-site determination of food contaminants: developments and applications, Microchem. J. 190 (2023) 108692, https://doi.org/10.1016/j.microc.2023.108692.
[2] S. Seetasang, M.I. Umeda, J. Ren, T. Kaneta, Innovations in paper-based analytical devices and portable absorption photometers for onsite analysis, Anal. Sci. 41 (2025) 1169–1184, doi:10.1007/s44211-025-00764-2.
[3] J. Zhang, Z. Zhou, B. Hu, Onsite environmental analysis by portable mass spectrometry, TrAC, Trends Anal. Chem. 193 (2025) 118461, https://doi.org/10.1016/j.trac.2025.118461.
[4] P.M. Kalligosfyri, S. Madani, A. Miglione, W. Cimmino, S. Cinti, A. Hatamie, Micro-analytical Lab-on-a-Tip: advances and perspectives, Anal. Chem. 97 (40) (2025) 21779–21792, https://doi.org/10.1021/acs.analchem.5c04914.
[5] Y. Liu, Z. Zhang, Y. Lin, J. Zhang, C. Zheng, Current trends of on-site analytical methods for organic contaminant determination in environmental waters, TrAC, Trends Anal. Chem. 194 (2026) 118553, https://doi.org/10.1016/j.trac.2025.118553.
[6] K.T. Lau, S. Baldwin, M. O'Toole, R. Shepherd, W.J. Yerazunis, S. Izuo, S. Ueyama, D. Diamond, A low-cost optical sensing device based on paired emitter–detector light emitting diodes, Anal. Chim. Acta 557 (1-2) (2006) 111–116, https://doi.org/10.1016/j.aca.2005.10.046.
[7] Ł. Tymecki, R. Koncki, Simplified paired-emitter–detector-diodes-based photometry with improved sensitivity, Anal. Chim. Acta 639 (1-2) (2009) 73–77, https://doi.org/10.1016/j.aca.2009.03.014.
[8] S. Seetasang, T. Kaneta, Development of a miniaturized photometer with paired emitter-detector light-emitting diodes for investigating thiocyanate levels in the saliva of smokers and non-smokers, Talanta 204 (2019) 586–591, https://doi.org/10.1016/j.talanta.2019.06.024.
[9] S. Seetasang, T. Kaneta, On-site analysis of paraquat using a completely portable photometric detector operated with small, rechargeable batteries, Anal. Chim. Acta 1135 (2020) 99–106, https://doi.org/10.1016/j.aca.2020.08.051.
[10] K. Danchana, V. Cerdà, Design of a portable spectrophotometric system part II: using a digital microscope as detector, Talanta 216 (2020) 120977, https://doi.org/10.1016/j.talanta.2020.120977.
[11] K. Danchana, P. Phansi, C.T. de Souza, S.L.C. Ferreira, V. Cerdà, Spectrophotometric system based on a device created by 3D printing for the accommodation of a webcam chamber as a detection system, Talanta 206 (2020) 120250, https://doi.org/10.1016/j.talanta.2019.120250.
[12] S. Seetasang, T. Kaneta, Portable two-color photometer based on paired light emitter detector diodes and its application to the determination of paraquat and diquat, Microchem. J. 171 (2021) 106777, https://doi.org/10.1016/j.microc.2021.106777.
[13] E.J. Könnel, S.D. Nonno, R. Ulber, Low-cost and easy-to-use: a portable photometer for simple and comprehensive analysis of critical water quality parameters, Microchem. J. 214 (2025) 113946, https://doi.org/10.1016/j.microc.2025.113946.
[14] A.W. Martinez, S.T. Phillips, M.J. Butte, G.M. Whitesides, Patterned paper as a platform for inexpensive, low-volume, portable bioassays, Angew. Chem. Int. Ed. 119 (8) (2007) 1340–1342, https://doi.org/10.1002/ange.200603817.
[15] G.G. Morbioli, T. Mazzu-Nascimento, A.M. Stockton, E. Carrilho, Technical aspects and challenges of colorimetric detection with microfluidic paper-based analytical devices (μPADs) - a review, Anal. Chim. Acta 970 (2017) 1–22, https://doi.org/10.1016/j.aca.2017.03.037.
[16] G.M. Fernandes, W.R. Silva, D.N. Barreto, R.S. Lamarca, P.C.F.L. Gomes, J.F. da S Petruci, A.D. Batista, Novel approaches for colorimetric measurements in analytical chemistry – a review, Anal. Chim. Acta 1135 (2020) 187–203, https://doi.org/10.1016/j.aca.2020.07.030.
[17] E. Noviana, T. Ozer, C.S. Carrell, J.S. Link, C. McMahon, I. Jang, C.S. Henry, Microfluidic paper-based analytical devices: from design to applications, Chem. Rev. 121 (19) (2021) 11835–11885, https://doi.org/10.1021/acs.chemrev.0c01335.
[18] D.M. Cate, W. Dungchai, J.C. Cunningham, J. Volckens, C.S. Henry, Simple, distance-based measurement for paper analytical devices, Lab Chip 13 (2013) 2397–2404, https://doi.org/10.1039/C3LC50072A.
[19] K. Yamada, T.G. Henares, K. Suzuki, D. Citterio, Distance-based tear lactoferrin assay on microfluidic paper device using interfacial interactions on surface-modified cellulose, ACS Appl. Mater. Interfaces 7 (44) (2015) 24864–24875, https://doi.org/10.1021/acsami.5b08124.
[20] X. Wei, T. Tian, S. Jia, Z. Zhu, Y. Ma, J. Sun, Z. Lin, C.J. Yang, Microfluidic distance readout sweet hydrogel integrated paper-based analytical device (μDiSH-PAD) for visual quantitative point-of-care testing, Anal. Chem. 88 (4) (2016) 2345–2352, https://doi.org/10.1021/acs.analchem.5b04294.
[21] Y. Shimada, T. Kaneta, Highly sensitive paper-based analytical devices with the introduction of a large-volume sample via continuous flow, Anal. Sci. 34 (2018) 65–70.
[22] K. Yamada, D. Citterio, C.S. Henry, "Dip-and-read" paper-based analytical devices using distance-based detection with color screening, Lab Chip 18 (2018) 1485–1493, https://doi.org/10.1039/C8LC00168E.
[23] C.T. Gerold, E. Bakker, C.S. Henry, Selective distance-based K^+ quantification on paper-based microfluidics, Anal. Chem. 90 (7) (2018) 4894–48900, https://doi.org/10.1021/acs.analchem.8b00559.
[24] N. Kohama, K. Matsuhira, T. Okazaki, K. Sazawa, N. Hata, H. Kuramitz, S. Taguchi, Colorimetric analysis based on solid-phase extraction with sedimentable dispersed particulates: demonstration of concept and application for on-site environmental water analysis, Anal. Bioanal. Chem. 414 (2022) 8389–8400, https://doi.org/10.1007/s00216-022-04375-y.
[25] N. Kohama, T. Okazaki, K. Sazawa, N. Hata, H. Kuramitz, S. Taguchi, Simple solid-phase colorimetry for trace Cr(VI) by combination of complexation with diphenylcarbazide and ion-pair solid-phase extraction with sedimentable dispersed particulates, Anal. Sci. 39 (2023) 857–865, https://doi.org/10.1007/s44211-023-00286-9.
[26] N. Kohama, T. Okazaki, K. Sazawa, N. Hata, H. Kuramitz, S. Taguchi, On-Site sensitive colorimetry for free cyanide by using ion-pair solid-phase extraction with sedimentable dispersed particulates and Mobile photography box, Molecules 29 (22) (2024) 5371, https://doi.org/10.3390/molecules29225371.
[27] N. Kohama, M. Kawahata, T. Okazaki, K. Sazawa, N. Hata, H. Kuramitz, S. Taguchi, Development of a simple visual and image-based colorimetric analytical method for Mn^{2+} using solid-phase extraction with sedimentable dispersed particulates, Microchem. J. 214 (2025) 114081, https://doi.org/10.1016/j.microc.2025.114081.
[28] I. Saar, H. Evard, Real-world implementation of particle-based microfluidics: on-spot test for iron and copper ions in water, ACS Omega 10 (1) (2025) 1800–1808, https://doi.org/10.1021/acsomega.4c10152.
[29] G. Wang, J. Li, S. Wu, T. Jiang, T.-H.A. Chen, Fully integrated, ready-to-use distance-based chemosensor for visual quantification of multiple heavy metal ions, Anal. Chem. 94 (46) (2022) 15925–15929, https://doi.org/10.1021/acs.analchem.2c04712.
[30] J. Ren, T. Kaneta, N-Benzoyl leucomethylene blue as a novel substrate for the assays of horseradish peroxidase by spectrophotometry and capillary electrophoresis–laser-induced fluorometry, Anal. Sci. 38 (2022) 651–655, https://doi.org/10.1007/s44211-022-00078-7.
[31] K. Danchana, H. Iwasaki, K. Ochiai, H. Namba, T. Kaneta, Determination of glutamate using paper-based microfluidic devices with colorimetric detection for food samples, Microchem. J. 179 (2022) 107513, https://doi.org/10.1016/j.microc.2022.107513.
[32] A.J.P. Martin, R.L.M. Synge, A new form of chromatogram employing two liquid phases, Biochem. J. 35 (12) (1941) 1358–1368, https://doi.org/10.1042/bj0351358.
[33] R.L. Burwell, R.G. Pearson, G.L. Haller, P.B. Tjok, S.P. Chock, The adsorption and reaction of coordination complexes on silica Gel, Inorg. Chem. 4 (8) (1965) 1123–1128, https://doi.org/10.1021/ic50030a008.
[34] T.T. Nguyen, T.H. Duy Nguyen, T.T. Thi Huynh, M.H. Dinh Dang, L.H. Thuy Nguyen, T. Le Hoang Doan, T.P. Nguyen, M.A. Nguyen, P.H. Tran, Ionic liquid-immobilized silica gel as a new sorbent for solid-phase extraction of heavy metal ions in water samples, RSC Adv. 12 (2022) 19741–19750, https://doi.org/10.1039/d2ra02980d.

[35] W.B. Fortune, M.G. Mellon, Determination of iron with o-phenanthroline: a spectrophotometric study, Ind. Eng. Chem. Anal. Ed. 10 (1938) 60–64, https://doi.org/10.1021/ac50118a004.
[36] A.C. Olivieri, Practical guidelines for reporting results in single- and multi-component analytical calibration: a tutorial, Anal. Chim. Acta 868 (2015) 10–22, https://doi.org/10.1016/j.aca.2015.01.017.
[37] D.M. Cate, S.D. Noblitt, J. Volckens, C.S. Henry, Multiplexed paper analytical device for quantification of metals using distance-based detection, Lab Chip 15 (2015) 2808–2818, https://doi.org/10.1039/C5LC00364D.